TOWARDS 'OPTIFLAP': PRELIMINARY STRUCTURAL SIZING METHODOLOGY FOR TRAILING-EDGE HIGH-LIFT SYSTEMS

R. Manikandan*, D. Zerbst*, E. Kappel*, L. Tönjes *, C. Hühne*

* German Aerospace Center (DLR), Institute of Lightweight Systems, Braunschweig, Germany

Abstract

This article proposes an efficient approach in preliminary sizing of composite flaperon structures using beam element solvers, in place of finite elements. Unlike traditional analyses that primarily address aerodynamic loading, the proposed methodology also accounts for kinematic failure load cases, enabling a more comprehensive assessment. A flaperon geometry—with varying cross-sections and thicknesses—is idealised into a beam element model with an appropriate node distribution. Structural responses to applied loads are then used by an optimisation process to size the structure, ensuring compliance with deflection, strain-failure, and buckling criteria. This streamlined workflow supports rapid trade studies, facilitating early identification of optimal design features and providing valuable insights during the preliminary design phase. The study demonstrates how this method can be applied to evaluate different material systems and highlights the lightweight benefits of spanwise thickness variation.

Keywords

flap design; beam-elements; cpacs

NOMENCLATURE

Formelzeichen

β	thickness scaling factor	
E	elastic modulus	GPa
G	shear modulus	GPa
n	critical failure load	N
ν	poisson's ratio	
ρ	material density	Kg/m^3
S	ultimate shear stress	MPa
t	laminate thickness	mm
θ	rotational degree of freedom	
u	translational degree of freedom	
X	ultimate lateral strength	MPa
Y	ultimate transverse strength	MPa

Indizes

AC	aircraft
Prepreg	pre-impregnated fiber layers
TE	trailing edge
UD	unidirectional

Abkürzungen

AMF	Advanced Multi-Spar Flap	
CAD	Computer Aided Design	
CFRP	Carbon Fibre Reinforced Plastics	
CMF	Composite Multi-Spar Flap	
CPACS	Common Parametric Aircraft Configuration Schema	
DLR	Deutsches Zentrum für Luft- und Raumfahrt	
FSD	Fully-Stressed Design	
HAR	High Aspect Ratio	
NTM	Normal-Transverse-Moment Aerodynamic Load envelope	N / Nm
PreDoCS	Preliminary Design of Composite Structures	
TRL	Technical Readiness Level	

1. INTRODUCTION

The development of next-generation single-aisle aircraft is centered around high-aspect-ratio (HAR) wings, a key-technology brick for reducing aerodynamic drag and enhancing fuel efficiency [1, 2]. However, these wings with longer spans and shallower cross-sections—introduce challenges to established designs and build philosophies, particularly for trailing-edge (TE) devices such as flaps. As seen in the DLR's HAR configuration (the F25, in Figure 1), the outboard regions are extremely slender with profile heights around 5–10 cm. Typically flaps are

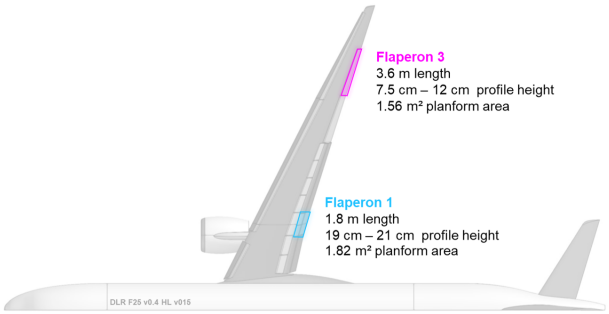

FIG 1. DLR F25 configuration - Data available on [3]

based on the differential or "skeleton" concept: a riveted assembly of CFRP ribs, spars, stiffened skins, and caps (the A321 standard, as seen in Figure 2). This concept becomes questionable when scaled-down for slender cross-sections and shrunk laminate regions, as established fastener-related parameters with edge-distance and pitch cannot be fulfilled. Moreover, these manufacturing philosophies, though proven for low-to-medium rates, become economically less feasible in high-rate production scenarios, as the industry targets rates of up to 100 AC/month. As such, this conventional concept faces limitations in both manufacturability and structural efficiency.

FIG 2. Differential concept (state of the art) © [4]

In response, the aerospace industry is exploring more integral design concepts to satisfy high production rate and assure the baseline requirement, that load-introduction fittings can be attached in an adequate way. Notable examples of such developments are shown in Figures 3a and 3b, which highlight results from high-TRL research activities. These CMF (Composite Multi-spar Flap) and AMF (Advanced Multi-cell Flap) designs are produced using dry-fiber preforms and resin transfer molding (RTM) processes. The driving motivation is to reduce cost, not only by reducing part count and fastener usage but also by simplifying assembly procedures.

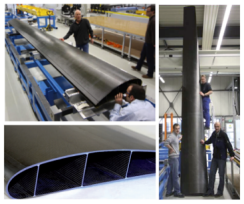

(a) More integral design, CMF, 2015 ©Radius [5]

(b) Advanced Multi-cell-flap, AMF, 2021 ©FACC [6]

(c) DLR omega-backbone concept 2024 (true scale)

FIG 3. High-TRL activities on composite flaps

Among the promising new concepts is DLR's Omega-backbone concept, shown in Figure 3c at true scale. This approach aims to provide structural continuity and load introduction capability in extremely shallow sections while reducing weight and assembly complexity. However, selecting the most suitable candidate for future HAR-wing applications—be it skeleton, multi-spar, or omega—requires the ability to quickly and consistently compare them during the preliminary design phase.

2. THE NEED FOR OPTIFLAP

As discussed, a variety of concepts exist for composite flaps, each with varying degrees of complexity, manufacturability, and structural performance. With the introduction of HAR-wings, these concepts must be critically evaluated to determine their viability under new geometric constraints and their potential to support low-cost, high-rate manufacturing. In response, we present a first step towards an integrated evaluation framework—OptiFlap—for comparative assessment of flap design concepts, early in the design phase.

Today, the typical design process selects a baseline concept early on, and then incrementally develop for technical readiness. This linear approach prevents thorough trade-off analyses between fundamentally unique concepts. As a result, important questions often go unanswered, including:

1) What is the best cross-section architecture for a flap of given size and aspect ratio?
2) How many spars are needed? What is their optimal position/arrangement?
3) How does material selection (e.g., prepreg vs. dry fiber) influence weight and stiffness?

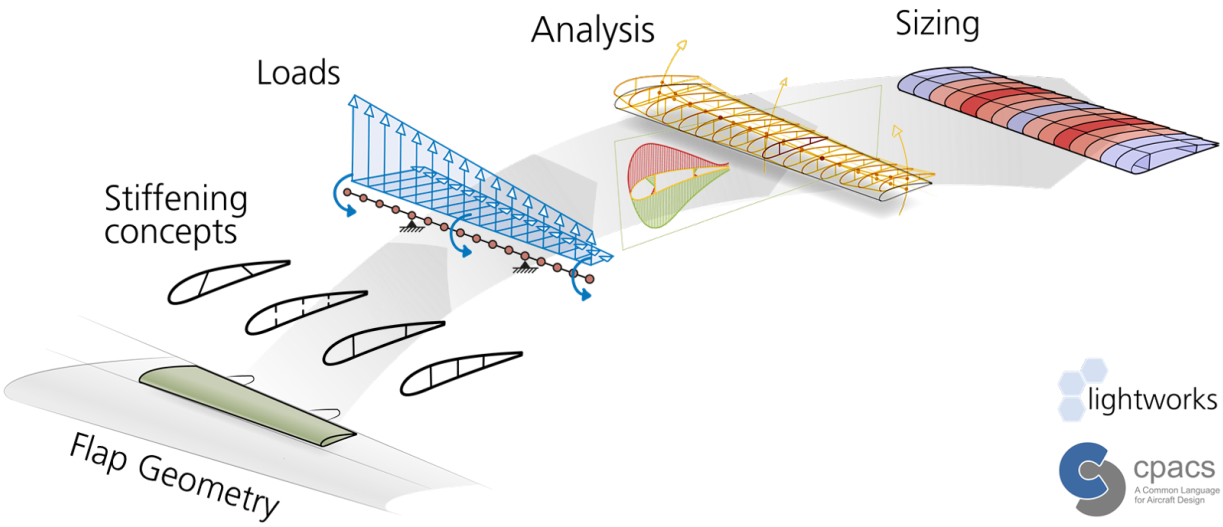

FIG 4. Overview of OptiFlap for preliminary design and analysis

4) Should spars be parallel or tilted to enable better attachment strategies?
5) Are separate designs required for inboard vs. outboard flaps? Or, can a unified concept work?
6) How many support stations are needed and what are their optimal positions?

These questions underscore the value of a focused preliminary design phase, where design flexibility is highest, before transitioning to detailed design. For example, spar spacing directly affects the width of laminate panels between them (buckling sensitive regions). Larger unsupported spans may require thicker (heavier) laminates to prevent instability. By introducing additional spars, laminate thickness can be reduced, but at the cost of added parts, increased assembly complexity, and reduced internal volume—particularly problematic for slender flap profiles where integration of load introduction points becomes more constrained. Furthermore, the placement of support stations along the span is critical from both structural and aerodynamic perspectives, as it influences the ability to control the gap between the wing and flap under load-induced deformation. These types of design questions and decisions illustrate the need for a tool that allows engineers to systematically vary design parameters and evaluate trade-offs across multiple performance metrics. OptiFlap shall support such concept evaluations based on quantifiable criteria such as weight, stiffness, manufacturability, and cost.

OptiFlap uses established methods of *lightworks*, DLR's in-house software, originally developed for multi-disciplinary and multi-fidelity optimisation of wings and rotor blades [7], and extends their capabilities for TE control surfaces, such as flaps or flaperons. By parameterising structural concepts (e.g., skeleton, multi-spar, omega-backbone) using the *CPACS* format [8], consistent evaluation criteria can be applied across all variants, by sizing them using a fast and efficient beam element solver. This data-driven approach to concept evaluation enables designers to quickly explore design alternatives, quantify trade-offs, and identify promising candidates for further development. In doing so, OptiFlap supports well-informed decisions in the preliminary design stage—balancing key drivers such as weight, stiffness, and subsequent material cost. The following section details the structure and processes within the proposed OptiFlap framework. To demonstrate the utility of this approach, two case studies will be shown to answer questions such as: the influence of allowing laminate-thickness variation across the components, and material selection.

3. DESIGN AND ANALYSIS USING OPTIFLAP

As illustrated in the overview (Figure 4), the design process begins with a parametric definition of the flap structure using a *CPACS* model. This allows for flexible control over geometric parameters—such as spar positions, the number of spars, and rib spacing—as well as structural attributes, including material assignments and design regions. Such a modelling approach supports rapid design iteration and preliminary studies.

From this input, an analysis model is automatically constructed using the beam-element solver of *lightworks* (*PreDoCS*-Preliminary Design of Composite Structures [9]), which represents the structure as an assembly of beam elements. Two load cases are considered here: the first simulates aerodynamic forces acting on the flap during flight, while the second represents a kinematic-lever failure scenario to assess compliance under off-nominal conditions. Based on the structural responses for these loads, *lightworks* uses a rapid sizing procedure to determine an optimal thickness distribution across the flap. For this study, the structure's stiffness is parameterised

as a homogenised quad laminate.

An overview of this process is provided in Figure 4, and detailed further in the following subsections.

3.1. Parametric Input Model

The flap model, used as input for the design procedure, is defined using the *CPACS* (Common Parametric Aircraft Configuration Schema) format [8]. The basic information required for the parametric representation of the flap is defined with respect to its geometry, structure, and applied load(s).

- **Geometry:** This includes the airfoil cross-section, planform dimensions (span and chord length), and position of reinforcement elements (e.g: spars). The airfoil profile is typically derived from a CAD file using a straightforward point-based method, as illustrated in Figure 5.

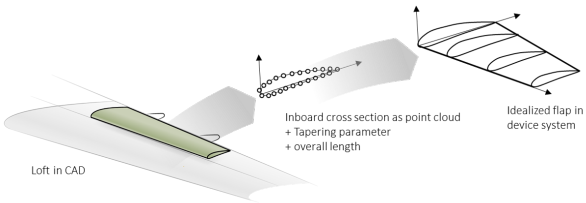

FIG 5. Airfoil geometry transfer from CAD

- **Structure:** This input includes the definition of composite material properties (E_1, E_2, ν_{12}, G_{12}), strength parameters (X, X_c, Y, Y_c, S), and density ρ). If thickness optimisation is to be performed, the sub-laminate used for sizing can be defined and assigned to distinct design regions on the skins and spars.
- **Loads:** Load definitions are specified along a reference axis, where force and moment vectors are applied. Appropriate boundary conditions are also defined at the support locations.

In this study, the position of the spars and kinematic attachment points followed standard design heuristics. An overview of the flap parameters considered is provided in Table 1.

TAB 1. Flap Parameters used in this study

Flaperon-3 of DLR F25 [3] (Version: wing v04, HL layout 015)	
Span	3.644 m
Min Chord Length	0.335 m
Max Chord Length	0.518 m
No. of Spars	2 (at 25% and 75% along chord length)
No. of Kinematic attachment points	2 (at 25% and 75% along span)

3.2. Load Cases and Boundary Conditions

To capture both nominal flight conditions and off-nominal scenarios, the following load cases

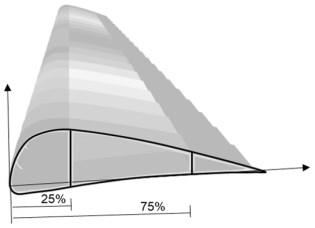

FIG 6. Chosen flap Cross section, with spars predefined at 25% and 75% chord

are evaluated for the flap.

Aerodynamic (NTM) load case: The Normal–Transverse– Moment (NTM) envelope for flaperon 3—summarised in Table 2—are based on several intact and failure cases from UP Wing project activities at the DLR [10]. These values are defined with respect to the leading edge, as seen in Figure 7. They are essential for the sizing of flap structures, fasteners, and load-introduction devices. These loads are applied as a linearly varying distribution along the span. The flaperon is held at 25% and 75% of the span by the actuation stations, which correspond to the clamped/fixed boundary condition points.

TAB 2. NTM loads used for Flaperon-3

N	T	M
65641 N	67 N	9730 Nm

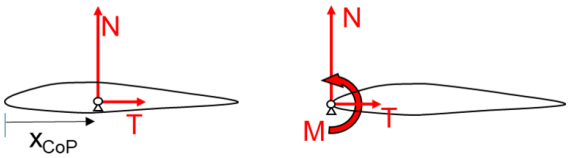

FIG 7. NTM-definition in LE-located device system, with $M = N \cdot x_{CoP}$

Kinematic-failure load case: As illustrated in Figure 8, this case simulates the failure of one actuator while the other(s) remains operational. Since the flaperon must still carry the full aerodynamic load through the operational actuators, the actuation loads are considered to be the complete aerodynamic M load (from Table 2). For each actuation station, a separate load case is analysed: the failed actuator is treated as fixed, and the M load is applied at the remaining operational actuator(s). For flaperon-3, which has two actuators, this results in two sub-cases. This load case ensures compliance of the structure even under actuator failure.

Each load case involves a distinct set of boundary conditions. The following subsections show how *lightworks* evaluates response of the flaperon for each case and size them appropriately.

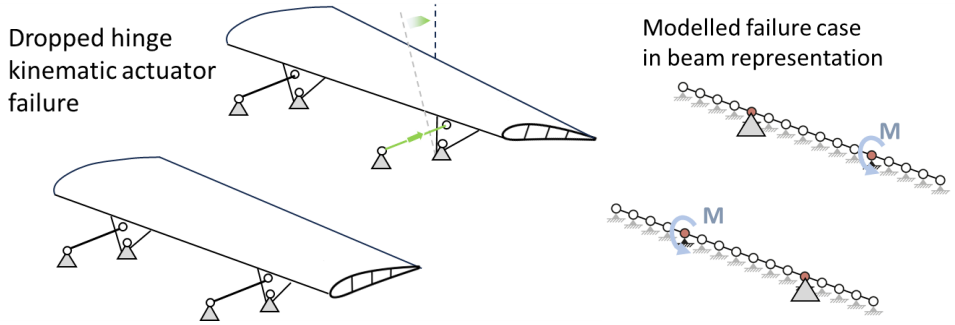

FIG 8. Dropped-Hinge kinematics, failure case and simplified modelling approach (see also: [11])

3.3. Mechanical Analysis using Beam Solver

The transformation of external loads into internal stresses is handled within the *PreDoCS* calculation scheme [9]. The flaperon structure is modeled using longitudinal beam elements, with stresses computed analytically at spanwise-discretised cross-sections. The *PreDoCS* model is automatically generated based on the geometry defined in the *CPACS* input file.

A key step in the calculation is determining the relationship between cross-sectional displacements and internal loads, expressed through the cross-sectional stiffness matrix. This matrix is derived using beam recovery relations applying Jung´s Theory, accounting not only for bending and extension but also shear and torsional effects. By integrating stresses (or strains) over the cross-section contour, the resulting force and moment fluxes on the structural components are obtained. These internal loads are then passed on to the design process to evaluate structural integrity.

To accurately capture the flaperon's tapering and structural response, the structure is discretised with 31 cross-sections across span. Hence, 30 beam elements were used in this study. The mounting of the flaperon at the kinematic attachment points is modeled through clamped boundary conditions applied to the respective nodes of the beam elements. In such clamped points, all translational and rotational degrees of freedom are fixed ($u_1 = u_2 = u_3 = \theta_1 = \theta_2 = \theta_3 = 0$).

3.4. Sizing with Fully Stressed Design Criteria

The flaperon structure is sized using the *lightworks* framework [12], which models each design region as a panel based on classical lamination theory. Internal loads computed by *PreDoCS* are mapped onto these panels to assess critical criteria such as buckling, strain, and if desired, even deflection.

Sizing follows the Fully Stressed Design (FSD) method [13], where the panel thickness t_i of the i^{th} panel is updated iteratively:

$$t_i^{(k+1)} = t_i^{(k)} \cdot \left(\frac{n_{\text{crit}}}{|n_i^{(k)}|} \right)^{\beta_i} \tag{1}$$

$$\beta_i = \begin{cases} \frac{1}{3}, & \text{buckling} \\ 1, & \text{strain, deflection} \end{cases} \tag{2}$$

Iterations continue until the objective converges within a tolerance of 1e-7, at which point the structure can be considered fully stressed: each panel operates near its allowable limit for the governing constraint (buckling, strain, or deflection) without exceeding it. Buckling behavior is predicted using analytical formulations from the HSB Handbook (provided in Appendix A). Strain limits are evaluated using the maximum-strain failure criterion, which ensures that the directional strains remain within allowable bounds of a given material.

In each step, thicknesses are scaled individually based on the maximum constraint violation in each region, among all load cases (as described in Section 3.2). To account for global deflection constraints—applied across all panels rather than locally—an extension of the standard FSD approach is employed. These constraints are introduced after an initial thickness distribution is established based on buckling and strain.

This sizing process is essentially thickness optimization. Here, each component is assigned a homogenized quad laminate/sublaminate, whose thickness is varied during sizing. All laminates considered here are symmetric and balanced to ensure manufacturability and predictable mechanical behavior.

For the skins, a 0° rich stacking sequence ($[45°, 90°, -45°, 0°, 0°]_S$) provides near quasi-isotropic behavior with enhanced axial stiffness. Spars, subject to shear-dominated loads, use a 45° dominant sequence ($[45°, -45°, -45°, 45°, 0°]_S$) while retaining some axial stiffness via 0° plies. Any alternative sublaminate can also be conveniently defined using the *CPACS* input, as for example, a sublaminate with a minimum of 10% ply count for 0°, $\pm 45°$ and $90°$ plies in the laminate.

4. TRADE STUDIES

With an efficient sizing tool in place, trade studies can be performed with ease. This helps understand how preliminary design decisions influence structural weight. To demonstrate the utility of this approach, two case studies are presented. The first explores how different levels of span-wise laminate-thickness variation influence resulting weight. The second explores the influence of material selection, comparing equivalent designs manufactured using dry fibre with RTM, and those using prepreg-based processes.

4.1. Varying number of laminate Design Regions

To study the impact of spanwise thickness variation, flaperon structures were designed with increasing number of design region along the spanwise direction—ranging from one up to 30—using a UD prepreg material M21EIMA (see Table 4 in Appendix for material properties).

As seen in Figure 9, with spanwise thickness variation, the sizing tool was able to use the material more efficiently, leading to a 14% reduction in structural weight. A design with no variation in thickness yielded a structural weight of 26.7 Kg. In contrast, a design incorporating spanwise thickness variation resulted in a weight of 22.85 Kgs. This highlights the benefit of allowing local tailoring to achieve lighter designs. The effect of incorporating thickness variation was most observed near the flaperon attachment points of the upper skin. For brevity, it is noted that the spars showed minimal thickness variation, with the rear spar showing none. The spar thicknesses ranged between 2 to 3 mm.

The results showed diminishing returns beyond 20 design regions, indicating convergence. The observed fluctuations in this mass convergence can be attributed to the FSD solver, which operates without gradient information for optimisation. As a result, the sizing process may converge to a local optimum.

The ability to vary laminate-thickness is closely linked to the chosen manufacturing process. For example, RTM typically requires solid metallic cores. In such cases, varying laminate-thickness can introduce undercuts in the part cavities, which necessitates multi-part core sectioning. Therefore, while thickness variation can yield lighter structures, the results from OptiFlap can be used to evaluate its practical applicability with respect to manufacturing constraints.

4.2. Varying material used

The second trade study evaluates the impact of material system selection. Here a flaperon was designed with spanwise thickness variation across 30 regions. The structure had already been sized using prepreg in the aforementioned study. For comparison, a dry fibre material (G0926 with RTM6 resin) was used to design an equivalent flap. To ensure a fair comparison, the dry-fibre design was constrained to meet the same maximum deflection as the prepreg design under in-service aerodynamic loads (capped at 3 mm).

Upon sizing with *lightworks*, the dry fibre-based structure resulted in a final weight of 25.94 Kg, compared to 22.85 Kg for the prepreg version. This 11% difference reflects the superior mechanical properties of the prepreg system, as summarised in Table 3.

TAB 3. Weight of Equivalent flaperon Structures made with different materials

Dry Fibre (G0926 RTM6)	Prepreg (M21EIMA)
25.84 Kgs	22.85 Kgs (-11%)

However, material selection is also driven by production cost. By assigning a cost-per-kilogram metric to each material, the proposed approach can be easily extended to provide a more holistic assessment, by estimating the material cost per flap. For brevity, the thickness distribution of the sized structure with dry fibre and prepreg are compared side-by-side in Figure 11 of the Appendix.

5. CONCLUSIONS

This work represents an initial step toward the OptiFlap framework- for preliminary structural sizing of TE high-lift systems. It starts with idealising a flap with varying cross-sections and thicknesses using beam elements with appropriate node distribution. Structural responses to given aerodynamic and kinematic loads are computed and fed into a sizing loop to ensure compliance with deflection, buckling, and strain-failure limits. This makes the approach well-suited for rapid trade studies, enabling early identification of promising design candidates and structural concepts. To demonstrate its utility, two key design questions were explored in the present manuscript:

1) Introducing spanwise laminate-thickness variation enabled a 14% reduction in structural weight, highlighting the benefits of not having a constant-thickness laminate in a critical load-carrying region.
2) Beyond 20 design regions, improvements in weight reduction plateaued, suggesting a practical limit for thickness variation in the preliminary design phase.
3) Material selection has a notable impact on structural performance, which can be quantified as a 11% weight-saving potential when using Prepreg-based designs (M21E/IMA UD) over dry-fibre (G0926/RTM6).

The current OptiFlap framework supports rapid trade studies using efficient beam models. Ongoing work explores alternative reinforcement concepts and optimising support-station position for flaps of varying aspect ratios (e.g., flaperon-1 and 3 on the

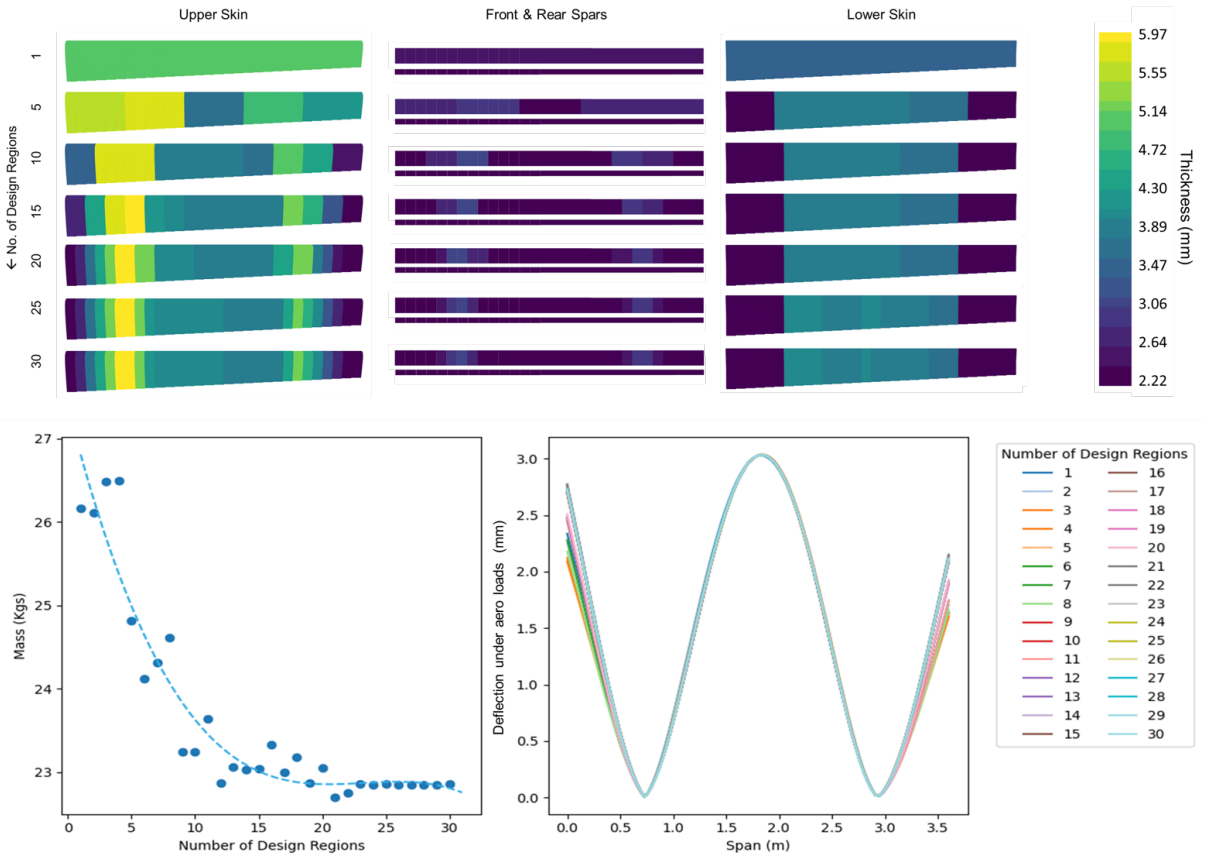

FIG 9. Thickness contours (top), mass convergence (bottom-left), and deflection under aero loads (bottom-right) of optimised flaps, with increasing number of laminate design regions (across span)

DLR F25). Future developments will increase model fidelity—integrating detailed FE simulations to refine load introduction strategies, such as the attachment design shown in Figure 10—positioning OptiFlap as a comprehensive design tool for next-generation TE high-lift devices.

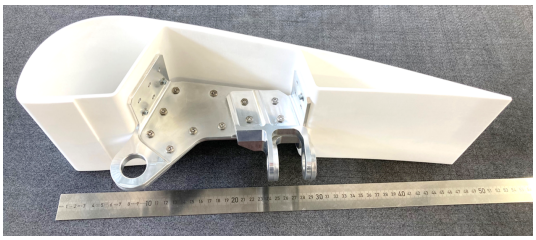

FIG 10. DLR's Omega-backbone-concept demonstrator, with integrated load introduction bracket, without closing bottom-skin underneath

Contact address:

rakshith.manikandan@dlr.de

References

[1] Allen Naomi. High aspect ratio wings – a critical technology for reaching net zero 2050. *Aerospace Technology Institute*, 2023. https://www.ati.org.uk/news/high-aspect-ratio-wings-a-critical-technology-for-reaching-net-zero-2050/.

[2] Dubois Thierry. Airbus progresses with folding-wing project. *Aviation Week Network*, 2023. https://aviationweek.com/air-transport/airbus-progresses-folding-wing-project.

[3] DLR. DLR research baseline F25, 2025. https://www.digital-hangar.de/portfolio/dlr-f25/.

[4] Ginger Gardiner. Reducing manufacturing cost via rtm. *CompositesWorld*, 2015. https://www.compositesworld.com/articles/reducing-manufacturing-cost-via-rtm.

[5] Radius Engineering. Airbus a320 outboard multi-spar flap. -, 2025. https://www.radiuseng.com/net_shape_composites#.

[6] Franz-Michael Sendner and Gernot Schneiderbauer. "wing of tomorrow": Facc und airbus entwickeln flügel der zukunft. -, 2021. https://www.facc.com/de/news/wing-of-tomorrow-facc-und-airbus-entwickeln-fluegel-der-zukunft/.

[7] Sascha Dähne, Edgar Werthen, David Zerbst, Lennart Tönjes, Hendrik Traub, and Christian Hühne. Lightworks, a scientific research framework for the design of stiffened composite-panel structures using gradient-based optimization. *Structural and Multidisciplinary Optimiza-*

tion, 67(5):70, May 2024. ISSN: 1615-1488. DOI: 10.1007/s00158-024-03783-1.

[8] M. Alder, E. Moerland, J. Jepsen, and B. Nagel. Recent Advances in Establishing a Common Language for Aircraft Design with CPACS. Technical report, DLR, 2020. DOI: https://elib.dlr.de/134341/.

[9] E. Werthen, D. Hardt, C. Balzani, and C. Hühne. Comparison of different cross-sectional approaches for the structural design and optimization of composite wind turbine blades based on beam models. *Wind Energy Science*, 9(7):1465–1481, 2024. DOI: 10.5194/wes-9-1465-2024.

[10] European Commission. Ultra-performing wing for sustainable and green air transport (upwing). https://doi.org/10.3030/101101974, 2023. Horizon Europe Project 101101974.

[11] Lerch M. and Thielecke F. Concepts for a safety device in conventional track-linkage kinematics to prevent skew in a single flap system. *Deutscher Luft- und Raumfahrtkongress (DLRK)*, (DocumentID: 450068), 2017.

[12] Sascha Dähne, Edgar Werthen, David Zerbst, Lennart Tönjes, Hendrik Traub, and Christian Hühne. Lightworks, a scientific research framework for the design of stiffened composite-panel structures using gradient-based optimization. *Structural and Multidisciplinary Optimization*, 67(5):70, May 2024. ISSN: 1615-1488. DOI: 10.1007/s00158-024-03783-1.

[13] Howard M. Adelman, Raphael T. Haftka, and Ilan Tsach. Application of fully stressed design procedures to redundant and non-isotropic structures. Technical Report NASA-TM-81842, NASA Langley Research Center, 1980. NASA Technical Memorandum 81842.

[14] Working Group Structural Analysis (IASB). *Aeronautical Engineering Handbook (LTH): Handbook for Structural Analysis (HSB)*.

A. BUCKLING FAILURE CRITERIA

The buckling behavior of the composite structure is assessed using analytical formulations from the HSB Handbook [14]. Critical loads for compressive and shear buckling are predicted separately using the following equations and subsequently combined using an appropriate interaction criterion.

Compression Buckling (HSB 45111-08)

For uniaxial compression, the critical load per unit width is given by:

$$n_{x,\text{cr}} = k_x\left(\bar{\alpha},\beta\right)\left(\frac{\pi}{b}\right)^2\sqrt{D_{11}D_{22}} \tag{3}$$

$$\bar{\alpha} = \frac{a}{b}\sqrt[4]{\frac{D_{22}}{D_{11}}}$$

$$\beta = \frac{D_{12}+2D_{66}}{\sqrt{D_{11}D_{22}}}$$

Here, x simply refers to the axis along which the highest principal load is observed.

Shear Buckling (HSB 45112-02)

For pure in-plane shear, the critical load per unit width is expressed as:

$$n_{s,\text{cr}} = k_s\left(\beta\right)\left(\frac{\pi}{b}\right)^2\sqrt[4]{D_{11}D_{22}^3} \tag{4}$$

Here, $D_{i,j}$ are components of the flexural stiffness matrix, and a and b represent a panel length and width, respectively The coefficients k_x and k_s are buckling coefficients, obtained from standard reference plots provided in the HSB Handbook. For combined loading scenarios (compression and shear), these critical loads are appropriately combined using the following relation:

$$R_x^2 + R_s^2 \leq 1 \tag{5}$$

Here, R, is defined as the the ratio between the applied loads and critical loads.

B. MATERIAL DATA

TAB 4. Material systems considered for design: Dry-fibre(left) and Prepreg(right)

	G0926 RTM6	M21EIMA
E_1 (GPa)	59.1	154
E_2 (GPa)	60.7	8.5
G_{12} (GPa)	3.8	4.2
ν_{12}	0.05	0.35
X_T (MPa)	718	2610
X_C (MPa)	710	1450
Y_T (MPa)	718	55
Y_C (MPa)	640	285
S (MPa)	115	105
ρ (Kg/m^3)	1600*	1580

C. SUPPLEMENTARY RESULTS

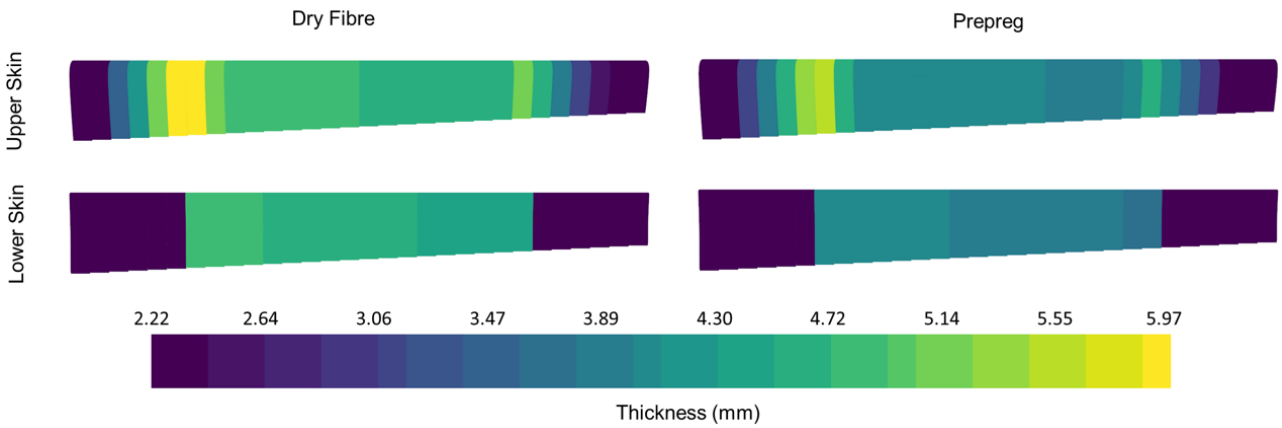

FIG 11. Sized flap structures with dry fibre(left), and prepreg(right)